Trajectory modification considering dynamic constraints of autonomous robots

Christoph Rösmann, Wendelin Feiten, Thomas Wösch
Siemens Corporate Technology, Intelligent Systems and Control, Germany

Frank Hoffmann, Torsten Bertram
Institute of Control Theory and Systems Engineering, Technische Universität Dortmund, Germany

Topic: **Research and Development** / modelling, planning and control
Keywords: Trajectory modification, timed elastic band, dynamics, kinematics, autonomous robots

Abstract

The classic "elastic band" deforms a path generated by a global planner with respect to the shortest path length while avoiding contact with obstacles. It does not take any dynamic constraints of the underlying robot into account directly. This contribution introduces a new approach called "timed elastic band" which explicitly considers temporal aspects of the motion in terms of dynamic constraints such as limited robot velocities and accelerations. The "timed elastic band" problem is formulated in a weighted multi-objective optimization framework. Most objectives are local as they depend on a few neighboring intermediate configurations. This results in a sparse system matrix for which efficient large-scale constrained least squares optimization methods exist.

Results from simulations and experiments with a real robot demonstrate that the approach is robust and computationally efficient to generate optimal robot trajectories in real time. The "timed elastic band" converts an initial path composed of a sequence of way points into a trajectory with explicit dependence on time which enables the control of the robot in real time. Due to its modular formulation the approach is easily extended to incorporate additional objectives and constraints.

1 Introduction

Motion planning is concerned with finding of a collision free trajectory that respects the kinematic and dynamic motion constraints.

In the context of motion planning this paper focuses on local path modification assuming that an initial path has been generated by a global planner [1]. In particular in the context of service robotics the modification of a path is a preferable approach due to the inherent uncertainty of the dynamic environment since the environment may be dynamic. Also, the model of the environment may subject to change due to partial, incomplete maps and dynamic obstacles. Furthermore, the (re-)computation of a large scale global path is often not feasible in real-time applications. This observation leads to approaches which modify a path locally, such as the "elastic band" proposed by [2, 3]. The main idea of the "elastic band" approach is to deform an originally given path by considering it as an elastic rubber band subject to internal and external forces which balance each other in the attempt to contract the path while keeping a distance from obstacles.

Later this approach was extended to non-holonomic kinematics [4, 5, 6], robotic systems with many degrees of freedom [7] and dynamics obstacles [8]. However, to our best knowledge dynamic motion constraints have not yet been considered as an objective in path deformation. The typical approach is to smoothen the path for example with splines to obtain dynamically feasible trajectories.
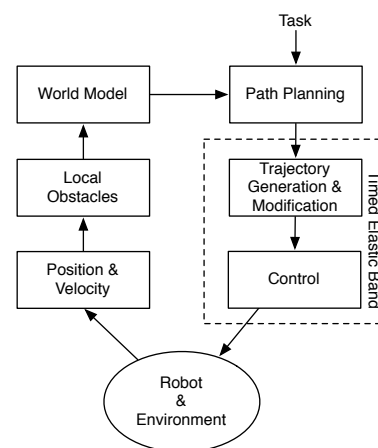

Figure 1: Robot system with "timed elastic band"

Our approach, called "timed elastic band" is novel as it explicitly augments "elastic band" with temporal information, thus allowing the consideration of the robot's dynamic constraints and direct modification of trajectories rather than paths. **Figure 1** shows the architecture of a robot system with the "timed elastic band". By considering the temporal information, the "timed elastic band" can be used to control also the velocites and accelerations of the robot. The new approach is suitable for high dimensional

state spaces even though this paper considers a differential drive mobile robot moving in a planar environment with three global and two local degrees of freedom.

2 Timed Elastic Band

The classic "elastic band" is described in terms of a sequence of n intermediate robot poses $\mathbf{x}_i = (x_i, y_i, \beta_i)^T \in \mathbb{R}^2 \times S^1$, in the following denoted as a configuration including position x_i, y_i and orientation β_i of the robot in the related frame ({map}, **Fig. 2**):

$$Q = \{\mathbf{x}_i\}_{i=0...n} \quad n \in \mathbb{N} \tag{1}$$

The "timed elastic band" (TEB) is augmented by the time intervals between two consecutive configurations, resulting in a sequence of $n-1$ time differences ΔT_i:

$$\tau = \{\Delta T_i\}_{i=0...n-1} \tag{2}$$

Each time difference denotes the time that the robot requires to transit from one configuration to the next configuration in sequence (Fig. 2). The TEB is defined as a tuple of both sequences:

$$B := (Q, \tau) \tag{3}$$

The key idea is to adapt and optimize the TEB in terms of both configurations and time intervals by a weighted multi-objective optimization in real-time:

$$f(B) = \sum_k \gamma_k f_k(B) \tag{4}$$

$$B^* = \underset{B}{\arg\min} f(B) \tag{5}$$

in which B^* denotes the optimized TEB, $f(B)$ denotes the objective function. In this paper it is a weighted sum of components f_k which capture the various aspects. This is the most elementary approach to multi-objective optimization, but already it yields very good results. In future work, more sophisticated approaches might be investigated.
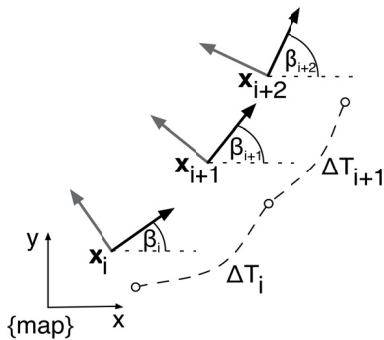
Figure 2: TEB: sequences of configurations and time differences

The majority of components of the objective function are local with respect to B as they only depend on a few number of consecutive configurations rather than the entire band. This property of locality of TEB results in a sparse system matrix, for which specialized fast and efficient large scale numerical optimization methods are available [11].

The objective functions of the TEB belong to two types: constraints such as velocity and acceleration limits formulated in terms of penalty functions and objectives with respect to trajectory such as shortest or fastest path (Eq. 18) or clearance from obstacles (Eq. 8). Sparse constrained optimization algorithms are not readily available in robotic frameworks (e.g. ROS) in a freely usable implementation. Therefore, in the context of "timed elastic band" these constraints are formulated as objectives in terms of a piecewise continuous, differentiable cost function that penalize the violation of a constraint (Eq. 6).

$$e_\Gamma(x, x_r, \epsilon, S, n) \simeq \begin{cases} (\frac{x-(x_r-\epsilon)}{S})^n & \text{if } x > x_r - \epsilon \\ 0 & \text{otherwise} \end{cases} \tag{6}$$

x_r denotes the bound. S, n and ϵ affect the accuracy of the approximation. Especially S expresses the scaling, n the polynomial order and ϵ a small translation of the approximation.
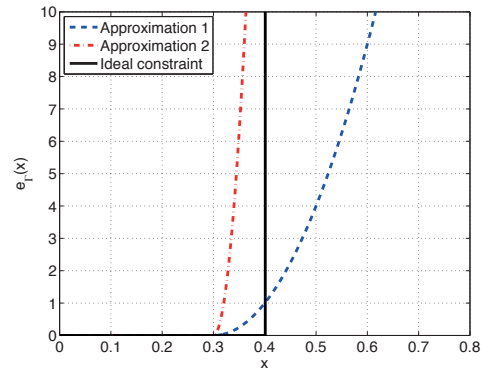
Figure 3: Polynomial approximation of constraints

Figure 3 shows two different realizations of Eq. 6. Approximation 1 results from parameter-set $n = 2$, $S = 0.1$, $\epsilon = 0.1$ and Approximation 2, which is conspicuously a stronger approximation, result from parameter-set $n = 2$, $S = 0.05$ and $\epsilon = 0.1$. This example shows an approximation of the constraint $x_r = 0.4$.

An obvious advantage of using a multi-objective optimization framework is the modular formulation of objective functions. The objective functions currently employed in the TEB are listed below.

2.1 Way points and obstacles

The TEB simultaneously accounts for the attainment of the intermediate way points of the original path and the avoid-

ance of static or dynamic obstacles. Both objective functions are similar with the difference that way points attract the elastic band whereas obstacles repel it. The objective function rests upon the minimal separation $d_{min,j}$ between the TEB and the way point or obstacle $\mathbf{z}_j$ (**Fig. 4**). In the case of way points the distance is bounded from above by a maximal target radius $r_{p_{max}}$ (Eq. 7) and in case of obstacles it is bounded from below by a minimal distance $r_{o_{min}}$ (Eq. 8). These constraints are implemented by the penalty function in Eq. 6.

$$
\begin{aligned}
f_{path} &= e_\Gamma(d_{min,j}, r_{p_{max}}, \epsilon, S, n) & (7) \\
f_{ob} &= e_\Gamma(-d_{min,j}, -r_{o_{min}}, \epsilon, S, n) & (8)
\end{aligned}
$$

According to Fig. 3, the signs of the separation $d_{min,j}$ and the bound $r_{o_{min}}$ in Eq. 8 must be swapped to realize a bounding from below.

Notice, that the gradient of these objective functions can be interpreted as an external force acting on the elastic band.
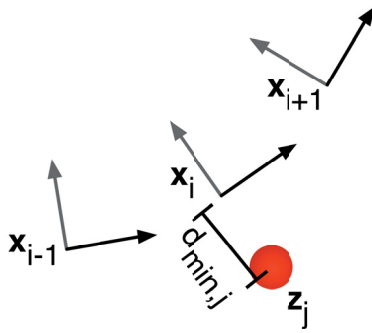

Figure 4: Minimal distance between TEB and way point or obstacle

2.2 Velocity and acceleration

Dynamic constraints on robot velocity and acceleration are described by similar penalty function as in the case of geometric constraints. Figure 2 shows the structure of TEB. The mean translational and rotational velocities are computed according to the euclidean or angular distance between two consecutive configurations $\mathbf{x}_i, \mathbf{x}_{i+1}$ and the time interval ΔT_i for the transition between both poses.

$$
\begin{aligned}
v_i &\simeq \frac{1}{\Delta T_i} \left\| \begin{pmatrix} x_{i+1} - x_i \\ y_{i+1} - y_i \end{pmatrix} \right\| & (9) \\
\omega_i &\simeq \frac{\beta_{i+1} - \beta_i}{\Delta T_i} & (10)
\end{aligned}
$$

Due to the vicinity of configurations the euclidean distance is a sufficient approximation of the true length of the circular path between two consecutive poses. The acceleration relates two consecutive mean velocities, thus considers three consecutive configurations with two corresponding time intervals:

$$
a_i = \frac{2(v_{i+1} - v_i)}{\Delta T_i + \Delta T_{i+1}} \qquad (11)
$$

For the sake of clarity, the three consecutive configurations are substituted by their two related velocities in Eq. 11. The rotational acceleration is computed similar to Eq. 11 by considering rotational velocities instead of translational ones. Considering a differential drive mobile robot, the relationship between the wheel velocities and the translational and rotational velocities v_i and ω_i of the robot center point are computed according to:

$$
\begin{aligned}
v_{w_r,i} &= v_i + L\omega_i & (12) \\
v_{w_l,i} &= v_i - L\omega_i & (13)
\end{aligned}
$$

in which the parameter L denotes half of the robot wheelbase.

Differentiating Eq. 12 and Eq. 13 with respect to time leads to the corresponding wheel accelerations. The wheel velocities and acceleration are bounded from above and below according to the manufacturer specifications. The translational and rotational inertia of the robot could be included in an obvious way, but in this first implementation we have not yet done so.
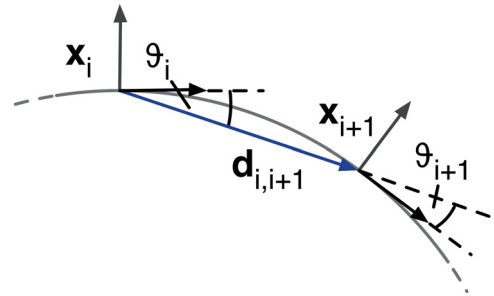
2.3 Non-holonomic kinematics

Figure 5: Relationship between configurations on a circle for non-holonomic kinematics

Robots with a differential drive only possess two local degrees of freedom. Thus they can only execute motions in the direction of the robot's current heading. This kinematic constraint leads to a smooth path that is composed of arc segments. Thus two adjacent configurations are required to be located on a common arc of constant curvature as illustrated in **Fig. 5**: The angle ϑ_i between the initial configuration $\mathbf{x}_i$ and the direction $\mathbf{d}_{i,i+1}$ has to be equal to the corresponding angle ϑ_{i+1} at the final configuration $\mathbf{x}_{i+1}$. If β_i denotes the absolute orientation of a robot at the i-th configuration the arc condition demands:

$$
\vartheta_i = \vartheta_{i+1} \qquad (14)
$$

$$
\Leftrightarrow \begin{pmatrix} \cos\beta_i \\ \sin\beta_i \\ 0 \end{pmatrix} \times \mathbf{d}_{i,i+1} = \mathbf{d}_{i,i+1} \times \begin{pmatrix} \cos\beta_{i+1} \\ \sin\beta_{i+1} \\ 0 \end{pmatrix} \quad (15)
$$

with the direction vector:

$$\mathbf{d}_{i,i+1} := \begin{pmatrix} x_{i+1} - x_i \\ y_{i+1} - y_i \\ 0 \end{pmatrix} \tag{16}$$

The corresponding objective function

$$f_k(\mathbf{x}_i, \mathbf{x}_{i+1}) = \left\| \left[\begin{pmatrix} \cos\beta_i \\ \sin\beta_i \\ 0 \end{pmatrix} + \begin{pmatrix} \cos\beta_{i+1} \\ \sin\beta_{i+1} \\ 0 \end{pmatrix} \right] \times \mathbf{d}_{i,i+1} \right\|^2 \tag{17}$$

penalizes the quadratic error in the violation of this constraint. A potential $180°$ orientation change is taken care of with an extra term.

2.4 Fastest path

Previous "elastic band" approaches obtain the shortest path by internal forces that contract the elastic band. Since our approach considers temporal information the objective of a shortest path we have the option to replace the objective of a shortest path with that of a fastest path, or to combine those objectives. The objective of a fastest path is easily achieved by minimizing the square of the sum of all time differences.

$$f_k = (\sum_{i=1}^{n} \Delta T_i)^2 \tag{18}$$

This objective leads to a fastest path in which the intermediate configurations are uniformly separated in time rather than space.

2.5 Implementation

Figure 6 shows the control flow of the implemented TEB. In the initialization-phase an initial path is enhanced to an initial trajectory by adding default timing information respecting the dynamic and kinematic constraints. In our case the initial trajectory is composed of piecewise linear segments with a pure rotation followed by a translation. Such a path representation in terms of a polygon is commonly provided by probabilistic roadmap planners [9]. Alternatively, Reeds-Shepp-paths are easily enhanced to admissible trajectories [10].

At each iteration, the algorithm dynamically adds new configurations or deletes previous ones in order to adjust the spatial and temporal resolution to the remaining trajectory length or planning horizon. A hysteresis is implemented to avoid oscillations. The optimization problem is transformed into a hyper-graph and solved with large scale optimization algorithms for sparse systems which are contained in the "g2o-framework" [11].
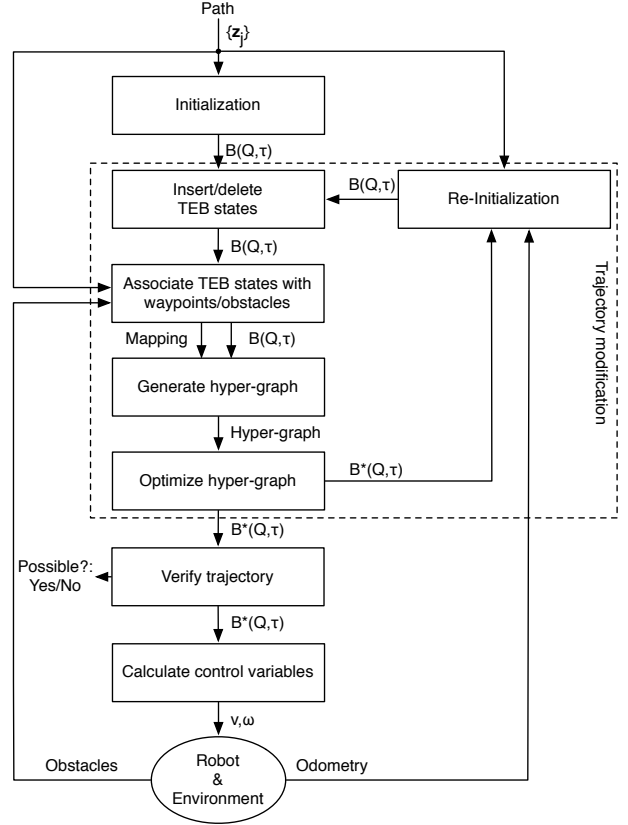

Figure 6: Control flow of TEB-implementation

The required hyper-graph is a graph in which the amount of connected nodes of one single edge is not limited. Therefore an edge can connect more than two nodes. The TEB problem (Eq. 4) can be transformed into a hyper-graph that has configurations and time differences as nodes. They are connected with edges representing given objective functions f_k or constraint functions. **Figure 7** shows an example hyper-graph with two configurations, one time difference and a point shaped obstacle. The velocity bounding objective function requires the mean velocity which relates to the euclidean distance between two configurations and the required travel time. Hence it forms an edge connecting those states of B. The obstacle requires one edge which is connected to the nearest configuration. The node representing the obstacle is fixed (double circle), thus its parameters (position) cannot be changed by optimization algorithms.

After verifying the optimized TEB, control variables v and ω can be calculated to directly command the robot drive system. Before every new iteration, the re-initialization-phase checks new and changing way-points which can be useful if way-points are received after analyzing short-range camera or laser-scan data.
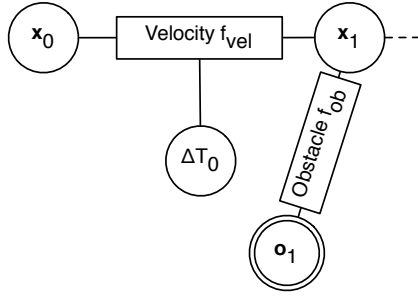
Figure 7: Velocity and obstacle objective function formulated as a hyper-graph

3   Experiments and results

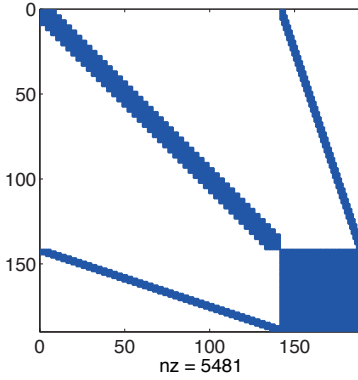In this section we give a short outline of the experimental results.

Figure 8: TEB: Sparse system-matrix of a TEB realization

As illustrated in **Fig. 8**, the resulting TEB system-matrix is still sparse with 15 percent of non-zero elements. In this example, the first 141 states corresponds to 47 configurations $\mathbf{x}_i$ and states 142-189 are the related time differences ΔT_i. Those last states are related to the objective function which aim is to achieve the fastest trajectory, thus this block is dense and grows quadratically with the dimension of the TEB.
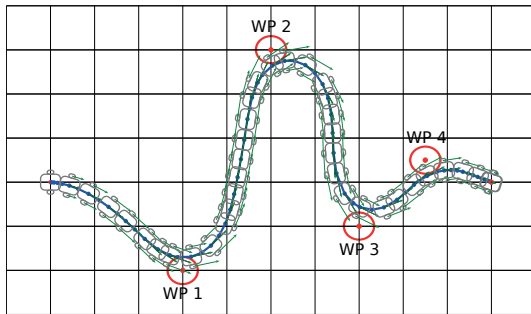

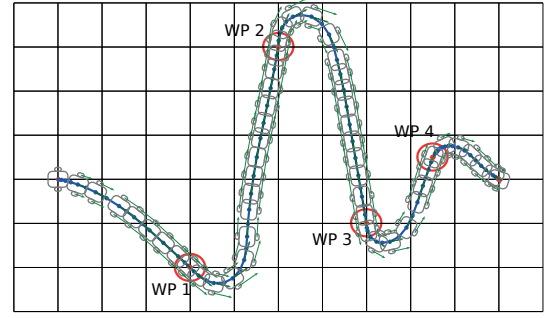**Figure 9:** Trajectory with way points: constraint approx. 1

Figure 10: Trajectory with way points: constraint approx. 2

Figure 9 and 10 show a scenario with four intermediate way points. In the second scenario, the TEB employs a stronger penalty for the violation of geometric constraints according to Fig. 3 (Approximation 2), thus robot traverses the way points more accurately. However, the solution that employs a weaker penalty for constraint violations often results in a smoother trajectory with less overshoot. Depending on the specific applications, tuning the weights allows for shifting the emphasis between a more accurate or a smoother and thereby faster trajectory. The dynamic limitations ($v_{max} = 1.4\,\frac{m}{s}$, $a_{max} = 0.4\,\frac{m}{s^2}$) are taken into account as shown in **Fig. 11**. A scenario with avoidance of static obstacles is illustrated in **Fig. 12**.
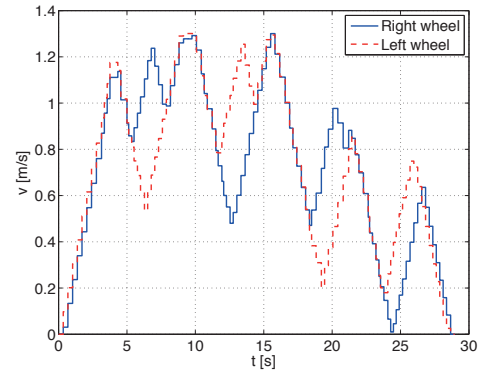

Figure 11: Velocity profile for scenario shown in fig.10

The augmentation of elastic bands with temporal information and the availability of efficient large scale optimizers for sparse systems allow for real-time trajectory adaptation and control of the robot.

Figure 13 shows a sequence of snapshots from an experiment with a Pioneer 2 robot in which a person walks through the scene. The Pioneer 2 is controlled by a Siemens Lifebook s6410 (Core2Duo, 2.4GHz, 2GBRAM) and is equipped with a Hokuyo Laser Scanner to detect the dynamic change of obstacle's position. The TEB adapts the original robots trajectory ($t = 0$) in real time and avoids an imminent collision with the person during the interval $t \in [6, 12]$ by stretching the trajectory away from the obstacle. The control cycle time is 25ms.
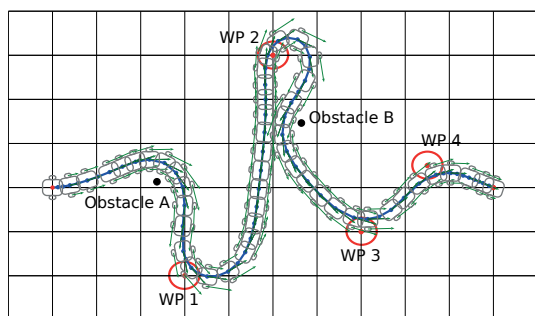
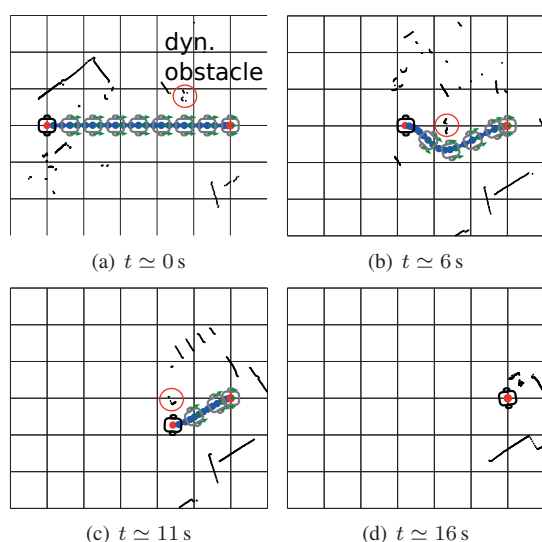**Figure 12:** Consider way points (Fig. 9) and obstacles

(a) $t \simeq 0\,\mathrm{s}$ (b) $t \simeq 6\,\mathrm{s}$

(c) $t \simeq 11\,\mathrm{s}$ (d) $t \simeq 16\,\mathrm{s}$

Figure 13: Avoiding a dynamic obstacle by real time adaptation of the TEB

4 Conclusion and further work

This paper presents a novel approach for real time trajectory modification with timed elastic bands. It rests upon the augmentation of the classic "elastic band" theory by temporal information. The proposed method makes it possible to not only to consider geometric constraints on the path but to simultaneously account for dynamic constraints of the mobile robot. The algorithm operates in real-time and thereby directly generates commands for the underlying robot motion controller. The method is highly flexible and is easily adapted to different robot kinematics and application requirements.

Future work is concerned with the development of a sparse constraint optimization framework, thus rendering the current formulation of constraints in terms of penalty functions obsolete. A different direction of research is to make the elastic band "jump over obstacles". Technically the approach is to surround an obstacle with a band with opposite orientation than the trajectory at the closest point, glue them at tangential point and cut the resulting trajectory at this point to obtain one that passes the obstacle on the other side. After optimizing this trajectory, it is decided on which side of the obstacle to continue. Note that this is still a local optimization, not guaranteed to find global optima.

References

[1] S. M. LaValle. *Planning Algorithms*, Cambridge University Press, Cambridge, U.K., 2006.

[2] Quinlan, S.; Khatib, O. *Elastic Bands: Connecting Path Planning and Control*, IEEE Int. Conf. on Robotics and Automation (ICRA) (2), 1993

[3] Quinlan, S. *Real-time modification of collision-free paths*, PhD thesis, Stanford University, 1994

[4] Khatib, M. *Sensor-based motion control for mobile robots*, Laboratoire d'Automatique et d'Analyse des Systèmes LAAS-CNRS, 1996

[5] Khatib, M. et al.*Dynamic Path Modification for Car-Like Nonholonomic Mobile Robots*, IEEE Int. Conf. on Robotics and Automation (ICRA), 1997

[6] Graf, B.; Wandosell, J.M.H.; Schaeffer, C. *Flexible Path Planning for Nonholonomic Mobile Robots*, Fraunhofer Institute Manufacturing Engineering and Automation (IPA), 2001

[7] Brock, O.; Khatib, O. *Executing Motion Plans for Robots with Many Degrees of Freedom in Dynamic Environments*, IEEE Int. Conf. on Robotics and Automation (ICRA), 1998, pp. 1-6

[8] Fiorini, P.; Shiller, Z. *Motion planning in dynamic environments using velocity obstacles*, International Journal on Robotics Research, Vol. 17, No. 7, July 1998, pp. 760-772

[9] Kavraki, L.E. et al. *Probabilistic roadmaps for path planning in high-dimensional configuration spaces*, IEEE Transactions on Robotics and Automation, Vol. 12, No.4, August 1996, pp.566-580

[10] Reeds, J.A.; Shepp L.A. *Optimal paths for a car that goes both forwards and backwards*, Pacific Journal of Mathematics, Vol. 145, No. 2, 1990, pp. 367-393

[11] Kümmerle, R. et al. *g2o: A General Framework for Graph Optimization*, Proc. of the IEEE Int. Conf. on Robotics and Automation (ICRA), May 2011